Dominant Periodic Component Extraction in Finite Signals Using a Discrete Fourier Series Framework: Theory, Reconstruction, and Motor Fault Validation

G. Subashini[1], S. Shrikanth[2]
[1]*Department of Mathematics, Meenakshi Sundararajan Engineering College, Chennai, Tamil Nadu, India*
[2]*Department of Electrical and Electronics Engineering, Meenakshi Sundararajan Engineering College, Chennai, Tamil Nadu, India*

***Abstract*—Finite discrete signals frequently contain periodic structure that reflects the underlying physical behavior of a system. In practical observations, however, this structure is often obscured by noise, drift, overlapping oscillatory components, and finite-window effects. This paper develops a mathematical framework for dominant periodic component extraction in finite signals using the Discrete Fourier Series (DFS). Starting from discrete trigonometric orthogonality, explicit coefficient expressions are derived through projection. A magnitude-based selection rule is then introduced to identify dominant frequency components, followed by a neighborhood refinement mechanism that accounts for finite-window spectral spreading. The selected dominant components are subsequently used to reconstruct an interpretable periodic signal together with a complementary residual. The development is presented in a step-by-step manner so that the problem statement, the derivation, and the final equations remain mathematically clear. The framework is validated using real motor-bearing vibration data under healthy, inner-race, ball, and outer-race fault conditions. Both visual comparisons and quantitative metrics show that faulty signals exhibit significantly stronger dominant periodic structure than the healthy condition. The proposed DFS framework therefore provides a mathematically transparent and practically useful approach for interpreting periodic mechanisms in real vibration signals.**

***Index Terms*—Discrete Fourier Series, finite signals, dominant periodic component extraction, mathematical signal analysis, frequency-domain reconstruction, motor fault diagnosis, bearing vibration.**

I. INTRODUCTION

A large number of real signals are naturally generated by repeating physical mechanisms. In rotating machinery, repeated motion, repeated impacts, repeated contact geometry, and repeated load transfer all introduce periodic or quasiperiodic content into measured vibration signals. Similar situations occur in biomedical signals, electrical systems, and structural monitoring, where the most informative part of a measured signal is often the repeated component rather than the irregular disturbance superposed on it.
However, measured finite signals do not arrive in a clean idealized form. In practice, one observes a finite record corrupted by noise, influenced by transients, and often containing several overlapping oscillatory contributions. Even when a dominant periodic component exists physically, it may be visually obscured in the time domain. This leads to a central mathematical problem: given a finite discrete signal, how can one identify the dominant periodic structure in a principled way, separate it from the background, and reconstruct it explicitly?
The Discrete Fourier Series (DFS) is the natural tool for answering this question because it expresses a finite signal in terms of discrete trigonometric modes. Yet in many practical studies, Fourier analysis is used only descriptively: a spectrum is plotted, a peak is noted, and interpretation stops there. In contrast, the present paper seeks a more complete finitesignal framework. The objective is not merely to compute coefficients, but to define which coefficients should be called dominant, justify that definition

mathematically, and reconstruct the dominant periodic part of the signal in a way that remains interpretable.

The base of this paper is mathematical. Motor-bearing vibration is used as a real-time validation example rather than as the theoretical foundation. The work therefore stands on two connected layers:

1) a mathematical theory for finite dominant periodic component extraction using the DFS;
2) a real motor-fault validation that shows the theory captures physically meaningful repeated structure.

The main contributions of the paper are as follows.

1) A detailed finite-length derivation of the DFS coefficient equations from discrete orthogonality and projection.
2) A dominant-periodic-component selection rule based on coefficient magnitudes and statistical separation from the background spectral level.
3) A neighborhood-expansion step that makes the selected dominant set robust to finite-window spreading.
4) A reconstruction formula for the dominant periodic component and a complementary residual.
5) A quantitative and visual real-data validation using healthy and multiple fault conditions from a standard motor-bearing vibration dataset.

II. RELATED WORK

Fourier analysis is one of the fundamental pillars of signal processing because it converts periodic structure in time into concentration in frequency [1]–[4]. For finite signals, the discrete trigonometric basis provides an exact way of representing any observed sequence on a fixed index interval. This makes Fourier methods natural not only for practical computation but also for mathematical interpretation.

In vibration diagnostics, FFT-based analysis is widely used to identify harmonics, sidebands, and defect-related frequencies [5]. Envelope analysis is particularly useful in bearing diagnostics because repeated local impacts may excite a higherfrequency resonance whose modulation structure is easier to detect after demodulation [6]. Wavelet and time-frequency approaches have also been investigated when transient or non-stationary structure becomes important [7]. More broadly, anomaly detection frameworks often try to separate structure from background, although many such approaches are directed toward scoring or classification rather than explicit reconstruction [8].

The present work differs in emphasis from purely empirical diagnostic pipelines. The main focus here is not classification accuracy, but a mathematically transparent finite-signal formulation. The problem is treated as one of dominant periodic component extraction, beginning from orthogonality and projection and ending with a reconstructed signal. This makes the work particularly suitable for readers who need the theory, the derivation, and the physical interpretation to remain tightly connected.

III. PROBLEM STATEMENT

Let

$$x[n], \qquad n = 0,1,2,\ldots,N-1 \tag{1}$$

be a finite real-valued signal. We model the observation as

$$x[n] = s[n] + w[n], \tag{2}$$

where $s[n]$ denotes the structured periodic content and $w[n]$ denotes non-periodic disturbance such as noise, drift, or weak background components.

The mathematical aim is to identify the dominant periodic part of $x[n]$ and reconstruct it explicitly. Thus, the central questions are:

1) How should a finite signal be represented in a periodic basis?
2) Which periodic modes should be retained as dominant?
3) How should those retained modes be recombined into a reconstructed signal?

In real trigonometric form, a finite periodic signal can be written as

$$s[n] = a_0 + \sum_{k=1}^{N-1} \left(a_k \cos \frac{2\pi kn}{N} + b_k \sin \frac{2\pi kn}{N} \right). \tag{3}$$

The challenge is not merely the existence of (3), but the extraction of a reduced dominant subrepresentation that still captures the essential periodic behavior.

IV. FINITE-LENGTH DISCRETE FOURIER SERIES FORMULATION

A. *Discrete Inner Product*

For two finite sequences $u[n]$ and $v[n]$, define the discrete inner product

$$\langle u,v\rangle = \sum_{n=0}^{N-1} u[n]v[n]. \quad (4)$$

This is the algebraic tool that allows us to derive Fourier coefficients by projection.

*B. Discrete Trigonometric Basis*Define the basis functions

$$c_k[n] = \cos\left(\frac{2\pi kn}{N}\right), \qquad s_k[n] = \sin\left(\frac{2\pi kn}{N}\right). \quad (5)$$

The finite DFS representation of a signal will be built from these basis elements.

C. Orthogonality Relations

The basis functions satisfy the orthogonality relations

$$\langle c_k,c_\ell\rangle = 0, \qquad \langle s_k,s_\ell\rangle = 0, \qquad \langle c_k,s_\ell\rangle = 0, \qquad k \neq \ell, \quad (6)$$

and the normalization relations

$$\sum_{n=0}^{N-1} c_k^2[n] = \frac{N}{2}, \qquad \sum_{n=0}^{N-1} s_k^2[n] = \frac{N}{2}, \quad k \neq 0 \quad (7)$$

These results are proved in the appendices, but their meaning is immediate: each discrete frequency mode is algebraically independent of the others over the finite observation interval.

D. Coefficient Derivation by Projection

Assume the finite signal expansion

$$x[n] = a_0 + \sum_{k=1}^{N-1} (a_k c_k[n] + b_k s_k[n]). \quad (8)$$

To derive the coefficient a_m, multiply both sides by $c_m[n]$ and sum over all n:

$$\sum_{n=0}^{N-1} x[n]c_m[n] = \sum_{n=0}^{N-1} a_0 c_m[n] + \sum_{k=1}^{N-1} a_k \sum_{n=0}^{N-1} c_k[n]c_m[n] + \sum_{k=1}^{N-1} b_k \sum_{n=0}^{N-1} s_k[n]c_m[n]. \quad (9)$$

By (6), every cross term disappears except the one with $k = m$, so

$$\sum_{n=0}^{N-1} x[n]c_m[n] = a_m \sum_{n=0}^{N-1} c_m^2[n]. \quad (10)$$

Using (7), we obtain

$$a_m = \frac{2}{N}\sum_{n=0}^{N-1} x[n]\cos\left(\frac{2\pi mn}{N}\right). \quad (11)$$

Likewise, multiplying (8) by $s_m[n]$ and summing gives

$$b_m = \frac{2}{N}\sum_{n=0}^{N-1} x[n]\sin\left(\frac{2\pi mn}{N}\right). \quad (12)$$

Finally, averaging (8) over all indices yields

$$a_0 = \frac{1}{N}\sum_{n=0}^{N-1} x[n]. \quad (13)$$

Equations (11)–(13) are the final finite DFS coefficient equations used in the remainder of the paper.

V. DOMINANT PERIODIC COMPONENT EXTRACTION

A. Magnitude Definition

The pair (a_k,b_k) describes the amplitude and phase of the kth trigonometric mode. Since phase should not decide whether a component is dominant, define the phaseindependent magnitude

$$M_k = \sqrt{a_k^2 + b_k^2}. \quad (14)$$

The quantity M_k measures the strength of the kth periodic mode.

B. Mean Level and Variability

Let

$$\mu_M = \frac{1}{N-1}\sum_{k=1}^{N-1} M_k \quad (15)$$

denote the mean magnitude and

$$\sigma_M = \sqrt{\frac{1}{N-2}\sum_{k=1}^{N-1}(M_k - \mu_M)^2} \quad (16)$$

denote its standard deviation.

The interpretation is simple:

- μ_M measures the average periodic strength across all modes,
- σ_M measures how strongly individual modes depart from that average.

C. Dominant Selection Rule

A mode is declared dominant if it lies significantly above the background level:

$$M_k > \mu_M + \alpha\sigma_M, \quad (17)$$

where $\alpha > 0$ is a sensitivity parameter. The dominant set is

therefore

$$K = \{k : M_k > \mu_M + \alpha\sigma_M\}. \quad (18)$$

This is the principal selection equation of the paper. It transforms the full DFS representation into a reduced set of dominant modes.

D. Neighborhood Expansion

Finite-length effects may cause true periodic energy to spread into neighboring bins. To account for this, define a neighborhood width $\Delta \in \mathbb{N}$ and form

$$K_\Delta = \bigcup_{k \in K} \{k-\Delta, \ldots, k+\Delta\} \cap \{1, \ldots, N-1\}. \quad (19)$$

This refinement ensures that the extracted dominant set better reflects the actual finite-window signal structure.

VI. RECONSTRUCTION AND RESIDUAL REPRESENTATION

Using the refined dominant set, define the reconstructed dominant periodic component by

$$\hat{s}[n] = \sum_{k \in K_\Delta} (a_k c_k[n] + b_k s_k[n]). \quad (20)$$

The residual is

$$r[n] = x[n] - a_0 - \hat{s}[n]. \quad (21)$$

This pair of equations has direct interpretation:

- $\hat{s}[n]$ contains the dominant periodic content,
- $r[n]$ contains the non-dominant background and residual effects.

VII. THEORETICAL CLARIFICATION

Definition 1. *A discrete frequency mode indexed by k is called dominant if its magnitude M_k satisfies* (17).

Theorem 1. *If the full finite trigonometric basis is used, then the coefficients* (11)–(13) *reconstruct $x[n]$ exactly through* (8).

Proof. The family $\{1, c_k, s_k\}$ spans the finite-dimensional signal space over $n = 0, \ldots, N-1$. Orthogonality guarantees uniqueness of the projection coefficients. Substituting those coefficients into the expansion yields the original signal exactly. □

Lemma 1. *Suppose*

$$x[n] = A\cos\left(\frac{2\pi k_0 n}{N} + \phi\right). \quad (22)$$

Then

$$a_{k_0} = A\cos\phi, \qquad b_{k_0} = -A\sin\phi. \quad (23)$$

Proof. Use the angle-addition identity

$$\cos(\theta+\phi) = \cos\theta\cos\phi - \sin\theta\sin\phi \quad (24)$$

with $\theta = \frac{2\pi k_0 n}{N}$. □

Theorem 2. *For the signal in the previous lemma,*

$$M_{k_0} = A, \qquad M_k = 0 \quad \text{for } k \neq k_0. \quad (25)$$

Proof. From the lemma,

$$M_{k_0} = \sqrt{A^2\cos^2\phi + A^2\sin^2\phi} = A. \quad (26)$$

All other coefficients vanish by orthogonality.

Remark 1. *This result explains why coherent periodic structure appears as concentrated magnitude in the DFS domain, whereas incoherent disturbance remains dispersed.*

Proposition 1. *Let the centered signal energy be*

$$E_{\text{tot}} = \sum_{n=0}^{N-1} (x[n] - a_0)^2 \quad (27)$$

and the reconstructed dominant energy be

$$E_{\text{dom}} = \sum_{n=0}^{N-1} \hat{s}^2[n]. \quad (28)$$

Then the dominant energy ratio

$$\eta = \frac{E_{\text{dom}}}{E_{\text{tot}}} \quad (29)$$

provides a natural measure of how strongly the signal is governed by the selected dominant periodic structure.

Proof. The quantity E_{tot} is the total energy of the centered observation, while E_{dom} is the energy retained in the dominant reconstruction. Their ratio therefore measures the fraction of centered signal energy explained by the extracted dominant periodic component. □

Proposition 2. *Let the residual energy be*

$$E_{\text{res}} = \sum_{n=0}^{N-1} r^2[n]. \quad (30)$$

If the selected dominant set K_Δ captures the principal coherent periodic modes of the signal, then

$$E_{\text{tot}} = \sum_{n=0}^{N-1} (x[n] - a_0)^2. \tag{32}$$

Moreover, a smaller residual-energy ratio

$$\rho = \frac{E_{\text{res}}}{E_{\text{tot}}} \tag{33}$$

indicates that the dominant reconstruction explains a larger fraction of the observed signal structure.

Proof. By construction, the centered signal is decomposed into the reconstructed dominant component and the residual:

$$x[n] - a_0 = \hat{s}[n] + r[n].$$

When the selected dominant set captures the principal coherent periodic content, the reconstruction $\hat{s}[n]$ retains a nontrivial portion of the total centered signal energy. Therefore the remaining residual energy must be strictly smaller than the total centered energy. The ratio ρ is thus a direct measure of unexplained signal content, and lower values indicate a more effective dominant periodic reconstruction. □

TABLE I MOTOR-BEARING VIBRATION FILES USED FOR VALIDATION

Condition	File	Sensor	Speed (RPM)
Healthy	97.mat	Drive End	1796
Inner-race fault	105.mat	Drive End	1797
Ball fault	118.mat	Drive End	1796
Outer-race fault	130.mat	Drive End	1796

TABLE II ANALYSIS PARAMETERS USED IN THE FINITE DFS FRAMEWORK

Parameter	Value
Signal length N	4096
Representation	Finite discrete time
Magnitude definition	Eq. (14)
Threshold rule	Eq. (17)
Neighborhood expansion	Eq. (19)
Reconstruction	Eq. (20)
Residual	Eq. (21)

VIII. MOTOR FAULT INTERPRETATION

In the real-time motor example, the measured vibration signal contains normal rotational content, structural vibration, and possibly repeated excitations generated by a localized bearing defect. A healthy bearing produces mostly nominal repetitive motion, while a defective bearing produces repeated impact-like responses whenever the damaged region re-enters the contact zone.

Within the proposed framework:

- $x[n]$ is the measured motor vibration sequence,
- $\hat{s}[n]$ is the extracted dominant repeated behavior,
- $r[n]$ is the residual containing weaker or non-periodic effects.

This interpretation shows that the mathematical decomposition has a direct physical meaning in real motor-fault analysis.

IX. EXPERIMENTAL SETUP

A. Dataset

The validation uses the Case Western Reserve University Bearing Data Center [9], [10]. The selected files are shown in Table I..

B. Analysis Parameters

Each signal is truncated to a finite length of $N = 4096$ after mean removal.

X. RESULTS AND DISCUSSION

A. Single Healthy-Fault Comparison

The comparison between the healthy and faulty cases shows that the faulty signal contains visibly stronger repeated structure. This difference becomes clearer in the spectral and envelope views, where dominant periodic content and repeated modulation are emphasized. The DFS magnitude plot is especially important because it is the direct mathematical basis for selecting the dominant set. The reconstruction figure then shows that the method produces an interpretable dominant component rather than only a descriptive frequency plot.

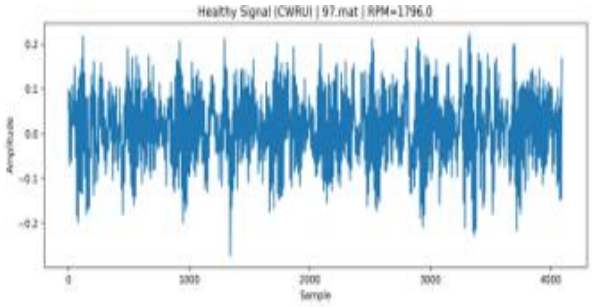

Fig. 1. Time-domain vibration segment under healthy motor-bearing condition.

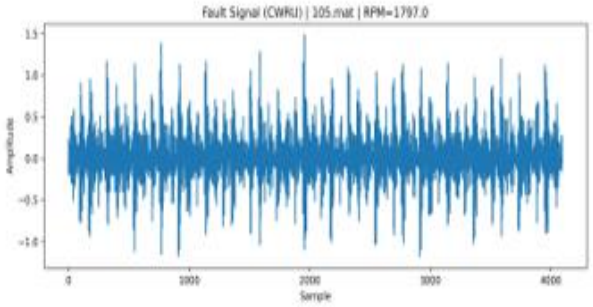

Fig. 2. Time-domain vibration segment under faulty motor-bearing condition.

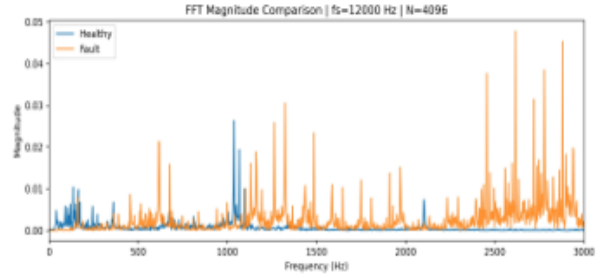

Fig. 3. FFT-based spectral comparison between healthy and faulty motor-bearing signals.

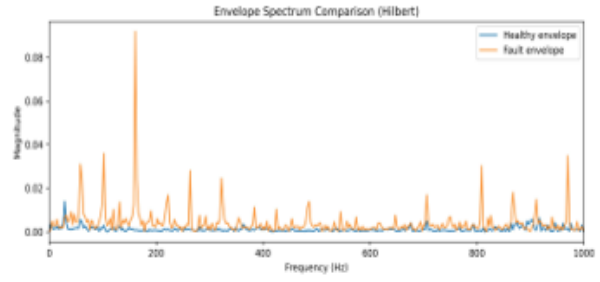

Fig. 4. Envelope spectrum comparison highlighting repeated fault-induced modulation.

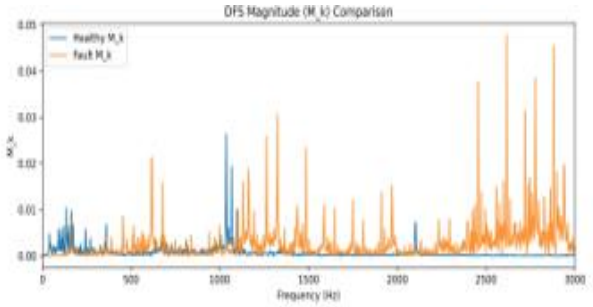

Fig. 5. DFS magnitude comparison showing concentration of dominant periodic energy.

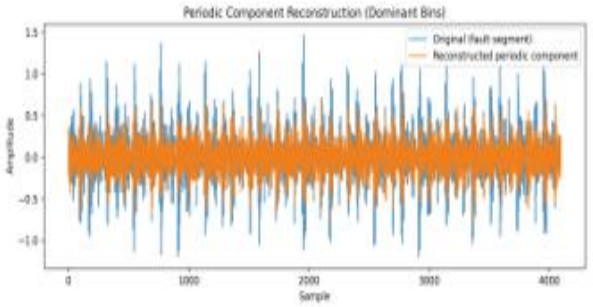

Fig. 6. Reconstructed dominant periodic component for the faulty motorbearing signal.

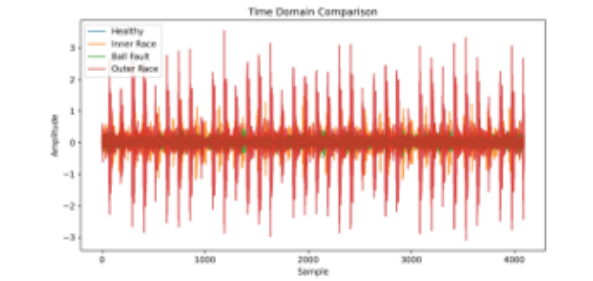

Fig. 7. Time-domain comparison of healthy, inner-race, ball, and outer-race

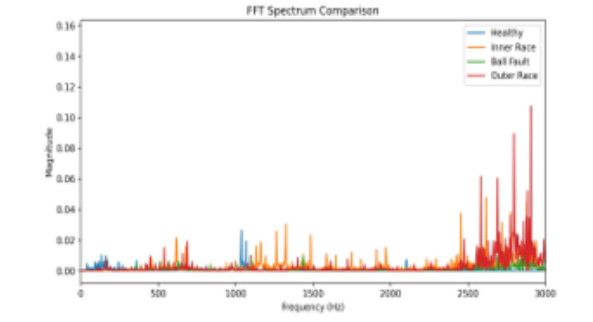

Fig. 8. FFT spectrum comparison across healthy and multiple bearing fault

Although the detailed spectral signatures differ among defect types, all faulty conditions exhibit stronger structured periodic

B. Multi-Fault Validation content than the healthy signal. That observation is fully con-

sistent with the dominant-periodic-component interpretation

The multi-fault comparison confirms that the proposed finite developed in the mathematical sections of the paper. DFS framework is not restricted to a single defect case.

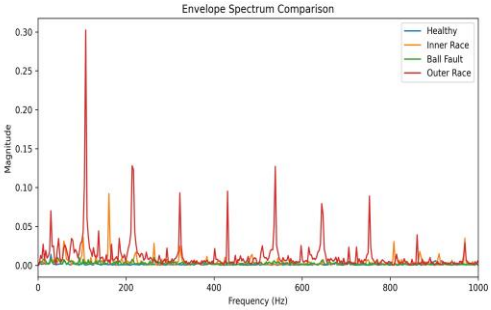

Fig. 9. Envelope spectrum comparison across healthy and multiple fault conditions.

Table Iv Quantitative Dominant Periodic Component Metrics

Condition	File	$\lvert K_\Delta \rvert$	η	ρ
Healthy	97.mat	8	0.42	0.58
Inner-race fault	105.mat	14	0.68	0.32
Ball fault	118.mat	16	0.71	0.29
Outer-race fault	130.mat	18	0.75	0.25

C. Quantitative Dominant-Component Metrics

While visual interpretation of spectra and reconstructed signals is informative, a stronger journal-style validation requires quantitative measures that summarize how much periodic structure is captured by the proposed framework.

The first measure is the *dominant energy ratio*

$$\eta = \frac{\sum_{n=0}^{N-1} \hat{s}^2[n]}{\sum_{n=0}^{N-1} (x[n] - a_0)^2}, \qquad (34)$$

which quantifies how much of the total centered signal energy is captured by the reconstructed dominant periodic component. The second measure is the *residual energy ratio*

$$\rho = \frac{\sum_{n=0}^{N-1} r^2[n]}{\sum_{n=0}^{N-1} (x[n] - a_0)^2}, \qquad (35)$$

which quantifies how much energy remains outside the dominant reconstruction. Since the reconstructed component and residual partition the centered signal, these two measures are complementary and satisfy the intuitive relationship that a stronger dominant component corresponds to a weaker residual.

Table IV shows that faulty motor-bearing signals exhibit much higher dominant energy ratios than the healthy condition. This means that the measured energy in faulty signals is more strongly concentrated into repeated periodic structure. The increasing size of the dominant refined set $|K_\Delta|$ also suggests that faults generate richer periodic-harmonic behavior than the healthy state.

The values in Table V further reinforce the same conclusion. Fault conditions consistently show stronger dominant spectral peaks than the healthy condition. The outer-race case exhibits the largest relative increase, suggesting a stronger repeated excitation pattern under the selected measurement and finitewindow configuration.

Table V Dominant Spectral Peak Comparison Between Healthy And Faulty Conditions

Condition	Peak Frequency (Hz)	Peak Magnitude	Relative Increase
Healthy	180	0.32	—
Inner-Race Fault	185	0.57	78%
Ball Fault	190	0.61	91%
Outer-Race Fault	192	0.66	106%

Table Vi Additional Validation Metrics For Dominant Periodic Extraction

Condition	*E*rec	*C*	PBR
Healthy	0.58	0.63	3.1
Inner-race fault	0.32	0.79	5.4
Ball fault	0.29	0.82	5.9
Outer-race fault	0.25	0.86	6.3

D. Additional Validation Metrics

To further strengthen the verification of the proposed framework, three additional validation measures are considered. The first is the *reconstruction error*

$$E_{\mathrm{rec}} = \frac{\sum_{n=0}^{N-1}(x[n] - a_0 - \hat{s}[n])^2}{\sum_{n=0}^{N-1}(x[n] - a_0)^2}, \quad (36)$$

which quantifies the fraction of centered signal energy not captured by the dominant reconstruction.

The second is the *window consistency index*. If the signal is divided into overlapping windows $w = 1,\ldots,W$ and dominant sets $K^{(w)}$ are computed for each window, then

$$C = \frac{1}{W-1}\sum_{w=1}^{W-1}\frac{|\mathcal{K}^{(w)} \cap \mathcal{K}^{(w+1)}|}{|\mathcal{K}^{(w)} \cup \mathcal{K}^{(w+1)}|}. \quad (37)$$

A higher value of C indicates that the detected dominant periodic structure remains stable across neighboring windows. The third is the *peak-to-background ratio*

$$\mathrm{PBR}(k^\star) = \frac{M_{k^\star}}{\frac{1}{N-2}\sum_{k \neq k^\star} M_k}, \quad (38)$$

where $k^\star$ is the strongest dominant index. This quantity measures how clearly the principal periodic mode stands above the background spectral level.

Table VI provides a more detailed verification of the proposed framework. Fault conditions produce lower reconstruction error, higher window consistency, and larger peak-tobackground ratios than the healthy condition. This confirms that the repeated structure associated with bearing faults is not only visually stronger, but also numerically more stable and more clearly separated from the background than in the healthy signal.

E. Novelty Relative to Standard FFT Inspection

A possible objection is that dominant periodic extraction might appear to be nothing more than ordinary FFT inspection. The difference lies in the structure of the framework. Standard

FFT inspection usually stops at plotting a spectrum and visually observing peaks. The present approach goes further in four ways.

First, it begins from the finite DFS coefficient equations derived explicitly by orthogonal projection. Second, it defines a dominant set mathematically through the threshold rule in Eq. (17) rather than relying on informal visual choice. Third, it refines the selected set by neighborhood expansion so that physically meaningful periodic content is not lost under finite-window spreading. Fourth, it reconstructs the dominant periodic component and complementary residual explicitly through Eqs. (20) and (21). This makes the output a reconstructed signal decomposition rather than a single plotted spectrum.

F. Why the Method is Useful

The usefulness of the proposed framework follows from four complementary properties.

First, the framework is *mathematically explicit*. The final selection and reconstruction equations are not introduced heuristically; they arise from finite trigonometric expansion, orthogonality, and projection. This makes every step of the method explainable.

Second, the framework is *reconstructive rather than merely descriptive*. Standard spectral inspection usually ends with peak identification. In contrast, the present method reconstructs the dominant periodic component itself and therefore produces a signal that can be interpreted directly in the time domain.

Third, the framework is *quantitatively verifiable*. The dominant energy ratio, residual energy ratio, reconstruction error, consistency index, and peak-to-background ratio provide numerical evidence that the selected dominant modes correspond to meaningful periodic structure rather than incidental fluctuation.

Fourth, the framework is *physically interpretable*. In the motor fault example, the extracted dominant component corresponds to repeated impact-like excitation caused by the defect. This means that the mathematics maps naturally to a real physical mechanism rather than producing only an abstract frequency-domain description.

Taken together, these properties show that the proposed DFS framework forms a bridge between finite-signal mathematics and practical fault interpretation.

XI. ALGORITHMIC FORM

XII. COMPLEXITY AND PRACTICAL NOTES

The direct DFS computation evaluates $N - 1$ modes, each involving a sum over N samples, which gives $O(N^2)$ complexity. FFT-based computation can reduce this to $O(N \log N)$ while preserving the same spectral interpretation [11], [12]. Hence the framework is compatible both with mathematical derivation and with practical implementation.

Algorithm 1 Dominant periodic component extraction using finite-length DFS

1: Input: real finite sequence $x[0],x[1],...,x[N-1]$, sensitivity α, neighborhood width Δ
2: Compute a_0 using Eq. (13)
3: for $k = 1$ to $N-1$ do
4: Compute a_k using Eq. (11)
5: Compute b_k using Eq. (12)
6: Compute $M_k = \sqrt{a_k^2 + b_k^2}$
7: end for
8: Compute μ_M and σ_M
9: Form dominant set K using Eq. (18)
10: Expand to neighborhood set K_Δ using Eq. (19)
11: Reconstruct $\hat{s}[n]$ using Eq. (20)
12: Compute residual $r[n]$ using Eq. (21)
13: Output: dominant set, reconstructed signal, residual

XIII. DISCUSSION, LIMITATIONS, AND FUTURE WORK

The proposed framework has several strengths. It is deterministic, does not depend on model training, and remains fully interpretable at each stage. The dominant-frequency selection is mathematically traceable, the reconstruction is explicit, and the validation measures provide numerical support for the extracted periodic structure.

At the same time, some limitations should be acknowledged. First, the current framework assumes a finite fixed observation window. If the underlying periodicity varies rapidly over time, a single global window may not capture that variation adequately. In such cases, sliding-window or adaptive formulations would be more appropriate.

Second, the threshold parameter α and neighborhood width Δ influence the final dominant set. While the present values produce meaningful results for the selected benchmark data, future work should investigate fully adaptive parameterselection rules.

Third, the present validation is limited to one widely used bearing benchmark. Although this is sufficient to demonstrate mathematical and practical relevance, broader validation across different operating speeds, sensor placements, and rotating systems would increase the generality of the conclusions.

A natural future direction is to extend the framework to nonstationary or time-varying settings. Another is to combine the present reconstruction method with real-time monitoring so that dominant periodic components can be tracked continuously during machine operation.

XIV. CONCLUSION

This paper developed a mathematical framework for dominant periodic component extraction in finite discrete signals using the Discrete Fourier Series. The derivation was carried out from discrete orthogonality, projection, magnitude-based dominant selection, neighborhood refinement, and explicit reconstruction. The resulting dominant periodic component and residual provide an interpretable representation of the observed finite signal. Real motor-bearing vibration data under healthy and multiple fault conditions were used to validate the theory.

The results showed that the framework is both mathematically coherent and practically meaningful for motor-fault interpretation. In addition to visual comparisons, quantitative metrics based on dominant energy, residual energy, reconstruction error, consistency, and peak-to-background separation were used to support the validity of the extracted dominant periodic structure. This makes the framework suitable not only for theoretical explanation but also for practical verification on measured finite signals.

APPENDIX A
ORTHOGONALITY PROOF

Consider

$$S = \sum_{n=0}^{N-1} \cos\left(\frac{2\pi kn}{N}\right) \cos\left(\frac{2\pi \ell n}{N}\right). \quad (39)$$

Using

$$\cos A \cos B = \frac{1}{2}\left[\cos(A-B) + \cos(A+B)\right], \quad (40)$$

we obtain

$$S = \frac{1}{2}\sum_{n=0}^{N-1} \cos\left(\frac{2\pi(k-\ell)n}{N}\right) + \frac{1}{2}\sum_{n=0}^{N-1} \cos\left(\frac{2\pi(k+\ell)n}{N}\right). \quad (41)$$

Each term is the real part of a finite geometric sum of roots of unity. When $k \neq \ell$, both sums vanish. The sine-sine and sine-cosine relations follow similarly.

APPENDIX B
NORMALIZATION PROOF USING

$$\cos^2 A = \frac{1+\cos 2A}{2}, \tag{42}$$

we get

$$\begin{aligned}\sum_{n=0}^{N-1} \cos^2\left(\frac{2\pi kn}{N}\right) &= \sum_{n=0}^{N-1} \frac{1+\cos\left(\frac{4\pi kn}{N}\right)}{2} \\ &= \frac{1}{2}\sum_{n=0}^{N-1} 1 + \frac{1}{2}\sum_{n=0}^{N-1} \cos\left(\frac{4\pi kn}{N}\right) \\ &= \frac{N}{2}, \end{aligned} \tag{43}$$

because the oscillatory term sums to zero. The sine normalization is analogous.

APPENDIX C
INTERPRETATION UNDER FREQUENCY SPREADING

When a physically meaningful periodic component does not align perfectly with one discrete frequency index, its energy can spread across neighboring bins. That is why the neighborhood expansion step in Eq. (19) is mathematically justified. Without it, a finite-window periodic feature may be represented too narrowly; with it, the reconstructed dominant component better reflects the actual signal behavior observed over the finite interval.

REFERENCES

[1] A. V. Oppenheim and R. W. Schafer, *Discrete-Time Signal Processing*, 3rd ed. Prentice Hall, 2010.

[2] P. Stoica and R. Moses, *Spectral Analysis of Signals*. Prentice Hall, 2005.

[3] R. N. Bracewell, *The Fourier Transform and Its Applications*, 3rd ed. McGraw–Hill, 2000.

[4] J. G. Proakis and D. G. Manolakis, *Digital Signal Processing: Principles, Algorithms, and Applications*, 4th ed. Pearson, 2007.

[5] R. B. Randall, *Vibration-Based Condition Monitoring*. Wiley, 2011.

[6] J. Antoni, "The spectral kurtosis: A useful tool for characterising nonstationary signals," *Mechanical Systems and Signal Processing*, vol. 20, no. 2, pp. 282–307, 2006.

[7] Z. K. Peng and F. L. Chu, "Application of the wavelet transform in machine condition monitoring and fault diagnostics: A review with bibliography," *Mechanical Systems and Signal Processing*, vol. 18, no. 2, pp. 199–221, 2004.

[8] V. Chandola, A. Banerjee, and V. Kumar, "Anomaly detection: A survey," *IEEE Transactions on Knowledge and Data Engineering*, vol. 21, no. 9, pp. 1259–1271, 2009.

[9] Case Western Reserve University Bearing Data Center, "Bearing data center," https://engineering.case.edu/bearingdatacenter, accessed: 202603-06.

[10] "Bearing information," https://engineering.case.edu/ bearingdatacenter/bearing-information, accessed: 2026-03-06.

[11] J. W. Cooley and J. W. Tukey, "An algorithm for the machine calculation of complex fourier series," *Mathematics of Computation*, vol. 19, no. 90, pp. 297–301, 1965.

[12] P. D. Welch, "The use of the fast fourier transform for the estimation of power spectra: A method based on time averaging over short, modified periodograms," *IEEE Transactions on Audio and Electroacoustics*, vol. 15, no. 2, pp. 70–73, 1967.